Agricultural and Forest Meteorology 336 (2023) 109471

Contents lists available at ScienceDirect

Agricultural and Forest Meteorology

journal homepage: www.elsevier.com/locate/agrformet

Estimating the response of Himalayan old-growth mountain forests to decreased monsoon precipitation

Norbu Wangdi [a,b,c,1], Iftekhar Uddin Ahmed [a,j,1], Mathias Mayer [a,d,e,1,*], Mani Prasad Nirola [f], Karma Orong [g], Norbu Zangmo [h], Douglas L. Godbold [a,i], Georg Gratzer [a], Andreas Schindlbacher [j]

[a] Institute of Forest Ecology, Department of Forest and Soil Sciences, University of Natural Resources and Life Sciences, A-1180,Vienna, Austria
[b] Bhutan Ecological Society, Thori Lam, Lower Changangkha, Thimphu, Bhutan
[c] Center for Climate and Sustainable Futures, School for Field Studies, Paro, Bhutan
[d] Forest Soils and Biogeochemistry, Swiss Federal Institute for Forest, Snow and Landscape Research (WSL), Zürcherstrasse 111, 8903 Birmensdorf, Switzerland
[e] Forest Ecology, Institute of Terrestrial Ecosystems (ITES), ETH Zurich, Universitätsstrasse 16, 8092 Zurich, Switzerland
[f] National Biodiversity Center, Serbithang, Bhutan
[g] Ugyen Wangchuck Institute for Forestry Research and Training, Department of Forests and Park Services, Lamai Goempa, Bumthang, Bhutan
[h] Divisional Forest Office, Department of Forests and Park Services, Zhemgang, Bhutan
[i] Department of Forest Protection and Wildlife Management, Faculty of Forestry and Wood Technology, Mendel University in Brno, Zemědělská 3, Brno, 613 00, Czech Republic
[j] Federal Research and Training Centre for Forests, Natural Hazards and Landscape – BFW, A-1131 Vienna, Austria

ARTICLE INFO

KEYWORDS:
Forest carbon
Monsoon failure
Drought
Soil CO_2 efflux
Fine roots biomass
Fine root production
Fine root decomposition
Water potential
Stem diameter growth

ABSTRACT

Forests in the Himalayas are a major carbon store, but are under threat due to changes in precipitation regime. To simulate a precipitation decline, throughfall-exclusion (TFE) shelters were applied during three consecutive monsoon seasons in an oak forest (2.650 m a.s.l.) and a conifer-dominated forest (3.260 m a.s.l.) in central Bhutan. Leaf water potentials, tree mortality, stem increment, soil CO_2 efflux, litterfall and fine root dynamics were assessed. TFE significantly and consistently decreased topsoil (0–30 cm) moisture and leaf water potentials of *Quercus lanata* and *Quercus griffithii* (lower elevation), and to a lesser extend those of *Tsuga dumosa* and *Quercus semecarpifolia*, (higher elevation). TFE did not impose tree mortality. Stem increment remained unaffected until the second TFE year, but showed reductions during the third year with *Tsuga dumosa* being most severely affected (-60%). Standing fine root biomass stocks were hardly affected by TFE. Increased root necromass and faster fine root growth in the lower elevation forest suggest that the oak trees increased C allocation below ground. Soil CO_2 efflux sharply declined during all three TFE years in both forests. Above ground litter input was unaffected by TFE until the second treatment year. Overall, both forest ecosystems appeared highly resistant to the imposed soil drying, with no signs of tree mortality and stable living root biomass stocks.

1. Introduction

Forest ecosystems in the eastern Himalayas (Nepal, Bhutan, India, China) represent a significant global carbon (C) pool, and the forests are ecologically, economically, and spiritually highly valued resources. Currently, forest structure and functions are being re-shaped by ongoing climate- and land use change (Dorji et al., 2019; Joshi and Joshi, 2019; Wangchuk et al., 2021). One key environmental factor affecting forest dynamics in the Himalayas is the amount and timing of monsoon precipitation. The South Asian summer monsoon provides water resources for the livelihood of around 20% of the global population and has shaped the landscapes, ecosystems and civilizations across Asia and the Himalayas (Kathayat et al., 2017). Though future precipitation scenarios hold high uncertainty, models overall suggest that climate change could make the Asian summer monsoon increasingly variable in time and space (Panthi et al., 2017; Singh et al., 2014, 2019) and that the probability of extreme events, such as total summer monsoon failures and subsequent extreme drought, could increase by the end of the 21st

* Correspondence author at: Swiss Federal Institute for Forest, Snow and Landscape Research (WSL), Zürcherstrasse 111, 8903 Birmensdorf, Switzerland.
E-mail addresses: mathias.mayer@wsl.ch, mathias_mayer@gmx.at (M. Mayer).
[1] Contributed equally to the publication

https://doi.org/10.1016/j.agrformet.2023.109471
Received 7 November 2022; Received in revised form 15 March 2023; Accepted 13 April 2023
Available online 24 April 2023
0168-1923/© 2023 The Author(s). Published by Elsevier B.V. This is an open access article under the CC BY license (http://creativecommons.org/licenses/by/4.0/).

century (Aadhar and Mishra, 2021; Menon et al., 2013; Preethi et al., 2019; Schewe and Levermann, 2012).

Located in the south-eastern foothills of the Himalaya massive, about 75% of Bhutan is covered by forests (Gilani et al., 2015). Mountain forests in Bhutan and the eastern Himalayan region have been shown to store high amounts of carbon (C) in biomass and soils, especially at mid- to high altitudes (Sharma and Rai, 2007; Simon et al., 2018; Tashi et al., 2016). Accordingly, they serve as important C sinks (FAO, 2010). Extreme drought events will strongly affect future forest C dynamics and stocks (van der Molen et al., 2011). Yet, it is unclear how and to which extent droughts affect forest functioning and C dynamics in this poorly studied and remote mountain region.

Drought affects forest ecosystem depending on its intensity, duration, timing, and frequency and is triggering an inter-linked response of various ecosystem components such as tree biomass, ground vegetation and soil (McDowell et al., 2022; Xu et al., 2020). To cope with, and to recover from drought stress, trees respond with a variety of complex interactive physiological above- and below ground processes (Adams et al., 2017; Brunner et al., 2015; Hartmann et al., 2018; Trugman et al., 2018). In the extreme case, drought causes tree mortality due to hydraulic failure, C starvation, or a combination of both (Adams et al., 2017; Arend et al., 2021; Bouyer et al., 2023). Tree mortality over a large area results in large post-disturbance ecosystem C losses from the decaying biomass and soils (Michaelian et al., 2011). To resist drought stress, trees reduce stomatal conductance, or shed leaves, which simultaneously reduces CO_2 uptake and tree growth (Martin-StPaul et al., 2017; McDowell et al., 2008). In this way, drought can substantially decrease the C uptake capacity of forested regions (Ciais et al., 2005).

Trees frequently respond to drought by adapting C allocation between above and below ground components (Trugman et al., 2018). To increase the ratio between water absorbing fine roots and transpiring leaf surfaces, tree species adapted to drier conditions tend to have higher root to shoot ratios (Joslin et al., 2000). However, there are no clear universal patterns on how different tree species respond to drought with regards to root production and activity (Brunner et al., 2015). Albeit that non-structural carbohydrate generally increases in fine roots during drought (Chuste et al., 2020; Ouyang et al., 2021), diverging fine root growth and turnover responses were observed between tree species and even among fine roots of the same species at different sites and drought preconditions (Fuchs et al., 2020; Meier and Leuschner, 2008; Nikolova et al., 2020). Conifers rely more on the existing roots than on the production of new roots during water stressed conditions (Mackay et al., 2020; Nikolova et al., 2020). The response of broadleaf trees, on the other hand, was shown to depend on the severity and duration of the drought, with trees reducing, maintaining, or increasing fine root biomass (summarized in Leuschner (2020)). Oaks, which also dominate the mid-elevation forests of the Eastern-Himalayas, were found to rather maintain or increase finer root biomass as a direct response to soil water stress (Chiatante et al., 2006; Di Iorio et al., 2011; Thomas and Gausling, 2000). However, these findings are mainly based on measurements on tree seedling/saplings from Mediterranean or temperate forests. The specific drought response of mature tree roots of the various forest types in the high altitudinal Monsoon climate of the eastern Himalayas is unknown.

Fine root C input is a key parameter determining how forest soils react to drought. The overall soil response to drought is determined by how soil C and nutrient inputs (leaf litter, root litter and exudation, microbial necromass) are affected, but also by how the soil biome (macro- to microorganisms) can cope with progressively drying soils. Microbial decomposer communities respond to water shortage by adapting growth and physiology, slowing down their metabolism, dying, or by entering into dormant stages (Bouskill et al., 2013; Fuchslueger et al., 2014; Göransson et al., 2013). This can impair plant nutrient supply and typically results in decreased organic matter decomposition and microbial respiration (heterotrophic soil CO_2 efflux) (Borken & Matzner, 2009; Schlesinger et al., 2016). Depending on the resilience of the soil microbiome, decomposer microbes can recover quickly after rewetting (Schimel, 2018), or drought leads to a sustained reduction of the soil CO_2 effluxes long after rewetting (Schindlbacher et al., 2012; Werner et al., 2021). The overall effect of drought on soil C therefore depends on how severe microbial activity is restricted by drought, how fast microorganisms recover during or after rewetting, and, in the longer-term, on the ability of microbes to adapt to dryer conditions (Borken et al., 2003; Rousk et al., 2013). The effects of reduced rainfall on soil C fluxes (C gain vs. loss) in Himalayan forests are still unclear. It yet remains open how different processes associated with soil C losses (e.g. soil organic matter decomposition) or soil C gains (e.g. fine root C inputs) are affected by soil drought. Since soils are huge C reservoirs in these forest ecosystems (Tashi et al., 2016), this knowledge is of great relevance to confine the sequestration potentials of atmospheric C.

This study aimed to understand how forests in the Eastern-Himalayas may respond to future droughts following monsoon failures. To that end, we established an artificial throughfall-exclusion (TFE) experiment in two representative forest types of Bhutan, a mixed oak forest at 2650 m a.s.l. and a mixed coniferous forest at 3250 m a.s.l., respectively. We studied processes and fluxes related to the forest C cycle, as they link above and below ground interactions representing an integrative measure of the whole ecosystem response to drought. In a recent review Pardos et al. (2021) showed that mixed forest stands, particularly with coniferous-broadleaved admixtures, exhibited a higher resilience to, and a faster recovery from drought than single species stands or broadleaved-broadleaved combinations. We therefore hypothesized that (1) high elevation mixed conifer forests will show a greater resistance (i.e. lower tree mortality and growth reductions) to drought than lower elevation mixed oak forests. We further hypothesized that (2) topsoil fine root biomass and -growth will increase in the mixed conifer forest as a response to drought, but they will be reduced in the oak forests, due to different resilience strategies among tree species; and (3) soil CO_2 efflux during drought periods will sharply decrease due to reduced microbial- and root activity. Overall, we expected negative drought effects on both ecosystem C uptake (tree mortality, growth) and ecosystem C loss (soil CO_2 efflux).

2. Materials and methods

2.1. Study sites and experimental setup

Located on the south slopes of the Himalayas, Bhutan is characterized by strong altitudinal gradients, ranging from more than 7000 m altitude in the North to around 120 m altitude in the South within a distance of around 150 km. Forest zones range from tropical and subtropical forests below 1000 m and 2000 m a.s.l., respectively, followed by warm-temperate and cool-temperate zones up to altitudes of 2500 and 3000 m altitude, respectively. The subalpine forest zone reaches up to around 4200 m a.s.l. (Ohsawa, 1987; Wangda and Ohsawa, 2006). Superimposed on these elevational zones are moisture gradients from mountain ranges open to the Indian plains to the innermontane valleys and, within valleys, from moist mountain slopes into dry valley bottoms (Wangda and Ohsawa, 2006). Taking these gradients into account, Wangda and Ohsawa (2006) classified forests in Western Bhutan into five zones, from a "warm, dry west Himalayan type" with *Pinus roxburghii* Sarg. below 1800 a.s.l. to "wide ranging cold conifer forests" dominated by *Abies densa* Griff. up to the treeline. The widest elevational range (1800 – 2550 m a.s.l.) is covered by the "wide ranging east-west Himalayan mixed broad-leaved type" dominated by oak species, followed by humid east Himalayan evergreen broad-leaved forests up to 2800 m a.s.l. and a cool humid east Himalayan conifer type dominated by *Tsuga dumosa* (D. Don.) Eichler and *A. densa* up to 3250 m altitude. In the latter zone, Simon et al. (2018) determined exceptionally high soil organic C stocks. We thus decided to study drought effects on ecosystem C dynamics in this zone as well as the zone with the widest elevational

distribution and the widest distribution across the Himalayan ranges, the "wide ranging east-west Himalayan mixed broad-leaved type".

The study took place in a cool mixed coniferous/hemlock dominated forest and a cool broadleaved oak forest, at Thimphu and Wangduephodrang district, Bhutan (Grierson and Long, 1983; Wikramanayake, 2002). Both sites experience a marked monsoon climate, with ~75% of the precipitation falling between June and September. The mixed conifer dominated forest was situated on a southeast facing slope close to the top of a mountain ridge nearby the Tashigang monastery (elevation 3260 m a.s.l). The mixed broadleaved forest was situated on an east facing gentle slope at the same mountain ridge ~11 km eastwards at lower elevation (2640 m a.s.l.) nearby the Pangsho monastery. Sites will be referred to as "Tashigang forest" and "Pangsho forest" in the further text. Both forests were never subject to planned logging operations. Both sites may have been subject to local forest use like fuelwood collection and maybe litter raking in the past. The site in Pangsho is in a relatively flat terrain and may have been used for agriculture more than at least a century years ago (judged from the size of trees established at the area).

Both forests were old growth stands. The Tashigang forest was dominated by *T. dumosa* along with *Picea spinulosa* Griff., *Quercus semecarpifolia* Sm. and *A. densa.* The Pangsho forest was dominated by *Quercus lanata* Sm. *and Quercus griffithii* Hk.. Soils at the Tashigang forest were Cambisols (WRB, 2006) on colluvial debris and on mica-schist bedrock. Soils at the Pangsho forest were Luvisols on quartzite bedrock. Soil organic C stocks (0–30 cm) are 142±25 and 96±28 t ha^{-1} in Tashigang and Pangsho forest, respectively (Wangdi et al., 2017). Basic stand parameters are provided in Table 1. A more detailed stand and soil description is given in Wangdi et al. (2017).

At each of the two forest sites, two 30×25 m roof structures were constructed out of bamboo in early 2014. The roof structures were covered with transparent plastic sheets, sheltering the whole soil surface area at a height of ~ 2.5 m above ground. Trenches of about 1.5 m depth were dug at the upper-slope edge of the roof constructions to hinder lateral influx of seepage water. During the first treatment year (2014), roofs were applied from the beginning of May till the end of August in order to simulate a strong reduction in monsoon precipitation. During the second (2015) and third (2016) study years, roofs were applied from mid-April until mid-October with the aim to simulate a total monsoon failure. A more detailed description of the roofs and the experimental set-up can be found in Wangdi et al. (2017).

2.2. Climate parameters

Site specific air temperature and precipitation data were derived from 1 km gridded climate data for Bhutan (Lehner and Formayer 2023).

Table 1
Stand characteristics for the control and the throughfall exclusion (TFE) sites prior to treatments in early 2014.

	Tashigang forest		Pangsho forest	
	Control	TFE	Control	TFE
Tree density (no. ha^{-1})	364 ± 70	438 ± 101	577 ± 25	758 ± 173
Tree height (m)	19.6 ± 13.0	20.5 ± 10.4	15.9 ± 9.1	12.2 ± 7.2
Tree dbh (cm)	40.5 ± 33.0	39.4 ± 26.4	25.6 ± 14.9	26.4 ± 17.7
LAI (leaf area index, $m^2\ m^{-2}$)	2.76	2.57	3.07	2.65
Tree basal area (m^2ha^{-1})	78.0 ± 7.4	77.7 ± 23.5	39.9 ± 6.2	54.8 ± 14.1
Standing volume (m^3ha^{-1})	1173 ± 1	1109 ± 387	464 ± 35	540 ± 116
Litter fall (t ha^{-1} yr^{-1})	7.0 ± 0.3	7.0 ± 1.6	6.8 ± 0.1	6.7 ± 0.9

Values are Mean ± SD wherever applicable.

Soil moisture (vol%) was measured manually at 0–20 cm soil depth using a portable handheld Field Scout TDR meter (Spectrum Technologies, Inc. Aurora, USA). Soil temperature (°C) was measured manually at 5 cm soil depth, using a handheld temperature probe (Hanna Instruments, USA). Manual soil moisture and temperature measurements were completed in the center of each 5 × 5 m control and treatment plot in parallel to soil CO_2 efflux measurements. Additionally, soil temperature and moisture were measured continuously at soil profile pits (four pits per forest type) with five combined soil temperature/soil moisture sensors (Decagon TM-5) at soil depths ranging from 5 to 120 cm. The data was recorded at 15 min intervals on a Decagon-Em50 data logger (Decagon Devices, Inc. USA). Soil moisture sensors were calibrated individually for representative soil layers (Wangdi et al., 2017).

2.3. Leaf water potential

Leaf water potential (Ψ, mid-day, 12:00) of 15 trees at the Tashigang forest (6 *T. dumosa*, 5 *Q. semecarpifolia* and 4 *R. arboreum*) and 20 trees at the Pangsho forest (7 *Q. lanata*,7 *Q. griffithii* and 6 *R. arboreum*) were measured using a portable Scholander pressure chamber (PMS 1515D, PMS Instrument Company, Albany, OR, USA) by removing three current-year leaves per tree from the upper canopy (25–35 m height) at eight occasions in 2015. Samples were collected from similar height of the individual target species and immediately placed in plastic bags to prevent further transpiration and thrown to the ground for immediate Ψ measurement. For reaching the canopies, fixed static ropes were installed at 25 trees in February 2015 and leaves were sampled from the same trees during all sampling dates.

2.4. Tree stem growth, tree mortality and above ground litterfall

Manual dendrometers (Environmental Measuring Systems, Brno, Czech Republic) were installed to measure radial stem growth. A total of 50 (29 at the Tashigang forest; 21 at the Pangsho forest) manual dendrometers were installed on the dominating tree species at breast height and the stem diameter was recorded once every three weeks. However, due to disturbances e.g. by bears, not all dendrometers produced reliable data. We therefore only used the undamaged dendrometers on dominating tree species (Tashigang forest: 22, Pangsho forest: 20) to estimate the average annual stem diameter increment of the corresponding forest sites and treatments.

Tree mortality was determined monthly by assessing defoliation status and crown transparency. The last assessment was conducted in April 2017. In the case of complete defoliation and no re-sprouting during the following year, a tree would have been considered as dead. Above ground litter was collected monthly (beginning in December 2014) using mesh-traps ($n = 20$) with an area of 1.0 m^2 (100×100 cm) placed within each roofed and control area in a five eye design of a dice. During roof application, litter collectors were placed above the roof surfaces. Litter dry weight was determined after drying at 80 °C. The C content of the above ground litter was estimated at 50% of the dry weight (De Wit et al., 2006). Litter that accumulated on the roof surfaces was regularly removed and evenly dispersed beneath the roofs. Frequent animal disturbance of litter sampling traps from 2016 onwards, resulted in inconsistencies and prevented a thorough comparison between TFE treatment and control. During 2015, above ground litterfall was consistently sampled at all plots, providing an un-biased estimate for this study year.

2.5. Fine root dynamics

Fine root (diameter ≤ 2 mm) biomass was estimated by soil coring (Makkonen and Helmisaari, 1999). The root sampling was carried out in May 2014 and April 2015, prior to roof application, as well as in August 2014 and October 2015 after roof removal by using a cylindrical soil corer (7.5 cm diameter, 30 cm depth). The core samples were taken from

each plot ($n = 10$ per forest site and treatment), and divided into three depth sections (0–10 cm, 10–20 cm, and 20–30 cm). After washing and sorting living roots and necromass, root samples were dried at 70 °C to constant mass. Elemental C in the dried root materials was determined with a LECO TruSpec CN elemental analyzer (Leco Corp., Saint Joseph, MI, USA).

Fine root production was estimated by the ingrowth core technique (Godbold et al., 2003; Lukac and Godbold, 2010) using a cylindrical mesh core (30 cm height and 6 cm diameter) allowing fine roots < 2 mm diameter to grow in. In May 2015, five mesh cores with root free soil (collected from the same spot) were placed into holes of previous root coring campaigns. After six months (October 2015), the cores were harvested and a second set of ingrowth cores was installed as before for the next six months growth (until April 2016). The cores were removed using a long sharp knife to detach the surrounding roots. All root materials (< 2 mm diameter) inside the mesh core were sorted, washed and dry mass was recorded as mentioned above. In rare cases, larger roots penetrated the mesh cores, these roots were discarded. Fine root turnover rate was calculated as annual root production divided by the mean standing biomass.

Fine root decomposition was estimated by the litter bag technique (Jamro et al., 2015) using nylon bags (10×10 cm) with a mesh size of 0.3 mm. Root samples of *Quercus* and *Tsuga* were collected from 0 to 10 cm soil depth of respective dominant forests, fine roots were then cut into 3–5 cm length and dried at room temperature. Each bag was filled with ~3 g of dried roots and sub-samples were retained to determine the moisture content and the chemical composition. In May 2014, a total of 160 litter bags (8 replicates × 5 time intervals × 2 treatments × 2 forest types) were randomly deployed in control and TFE areas and were buried at 5 cm mineral soil depth. Sixteen litter bags were retrieved from each forest after 3, 6, 12, 18, and 24 months, respectively. Decomposing roots were cleaned and then oven-dried at 70 °C to constant weight to determine the weight loss and for elemental C and N analyses.

2.6. Soil CO_2 efflux

Soil CO_2 efflux (= soil respiration; Rs) was surveyed regularly at the two forest types once every three weeks, from May until December 2014, from April until November 2015, and from May until December 2016. The replication was 10 plots per treatment (TFE, control) at each forest site. To cover the within-plot variability, four subplots were set along the cardinal directions, at about 150 cm from the plot center (total 40 subplots per forest type) and a mean plot value was calculated for further analyses. We used a portable infrared gas analyzer (EGM-4, PP-Systems, Amesbury, USA) with an attached soil respiration chamber (SRC-1, PP-Systems, Amesbury, USA) for Rs measurements. Subplots were equipped with permanent plastic collars (total height 5 cm, 2–3 cm inserted into the soil, diameter 10 cm) in spring 2015; collars thereafter served as permanent bases for Rs measurements. Due to logistical reasons, base collars for Rs measurements were not available in 2014. During the 2014 season, the chamber was directly placed on the ground surface and slightly pressed into the forest floor to produce a sufficient sealing. Soil CO_2 efflux was estimated by fitting a linear regression to the increasing headspace CO_2 concentration (chamber closure time 90 s). Each Rs measurement campaign lasted for ~ 5 h at each forest type. Measurements were carried out fully randomly to avoid any bias due to the dial variations in Rs.

2.7. Data analyses

The effect of TFE on fine root biomass C was assessed by means of two-way analysis of variance (ANOVA) with a nested model structure, where soil depth (0–10, 10–20 and 20–30 cm) was nested within plots. Independent sample *t*-test was used to compare between control and TFE of fine root necromass C, fine root production and turnover. A two compartment decay model was used to evaluate fine root decomposition rates (Rovira and Rovira, 2010):

$$X_t = ae - k_1^t + be - K_2^t \quad (1)$$

where a is the labile or initially decomposable part of the root litter, K_1 is the initial decay rate and b is the more resistant material with its decay rate K_2. Decay constant after time t, Kt was calculated as

$$Kt = Ln(Wt / W0)/t \quad (2)$$

Wt and W0 are mass of initial root litter and mass after time t, respectively. The effect of TFE on fine root decay rates and fine root production was assessed by means of independent sample t-tests.

The effects of TFE on Ψ, Rs, soil temperature and soil moisture were tested by applying an ANOVA with mixed effects model structure to account for a repeated measurement structure within the data (Pinheiro and Bates, 2000). Treatments were considered fixed effects and trees (for Ψ measurements) and plots (for Rs measurements) were considered random effects.

Linear mixed effect models were used to predict Rs as a function of soil temperature (Mayer et al., 2020). Due to an exponential relationship between Rs and soil temperature (Wangdi et al., 2017), data were log transformed prior to analysis. Fixed effects model coefficients are given in Table S1. Variables plots and year were assigned random effects; years were nested within plots. Random intercepts and slope coefficients were estimated for the response to soil temperature for each plot and year. Since seasonal soil temperature and moisture data were highly correlated across sites and treatments (cool and dry winter months and warm and wet summer months) the Rs models were not improved by including an additional soil moisture term (Reichstein and Beer, 2008).

The random effect part of the model (Table S1) and continuously measured soil temperature data were used to predict log(Rs) for each plot and day. The log(Rs) predictions were transformed to Rs by taking the exponent and an annual efflux sum was calculated.

Statistical analysis, modeling, and plotting were done in R, version 3.4.3 (R Core Team, 2017) and SPSS 16.0 (SPSS Inc., Chicago, IL). Used R packages were 'nlme' (J. Pinheiro et al., 2014) and 'MuMIn' (Barton, 2018). Level of significance for statistical analyses was a p-value <0.05.

3. Results

3.1. Climate and soil micro-climate

Air temperature and precipitation throughout the study period showed little variability between study years and were comparable to long-term (1996–2019) records (Fig. S1). In Pangsho, monthly air temperature ranged between −3.5 and 26.6 °C and precipitation ranged between 0 and 279 mm. In Tashigang, monthly air temperature ranged between −11.8 and 24.0 °C and precipitation ranged between 0 and 347 mm. In 2015 and 2016, average annual soil temperature was 13.6 and 13.3 °C at Pangsho forest control plots, and 10.3 and 10.5 °C at Tashigang forest control plots, respectively. Throughfall exclusion had no effect on soil temperature at both sites. In 2014, 2015, and 2016, average soil moisture at 5 cm soil depth was 37.4, 37.9, and 38.3 vol% at Pangsho control plots, and 31.2, 35.1, and 35.0 vol% at Tashigang forest control plots, respectively. Soil moisture was significantly reduced by TFE treatments at both sites: in Pangsho forest, soil moisture decreased by on average 6.8, 9.3, and 12.1 vol%, and in Tashigang forest it decreased by on average 5.5, 12.5, and 16.2 vol%, respectively.

3.2. Leaf water potentials

In 2015, the second year of TFE, Ψ ranged on average between −2.1 and −1.1 MPa in Pangsho forest control plots and between −1.9 and −0.9 MPa in Tashigang forest control plots (Fig. 1), respectively. The Ψ was significantly ($p < 0.001$) reduced by TFE treatments at both sites: in Pangsho forest, Ψ decreased down to −2.5 MPa, and in Tashigang forest

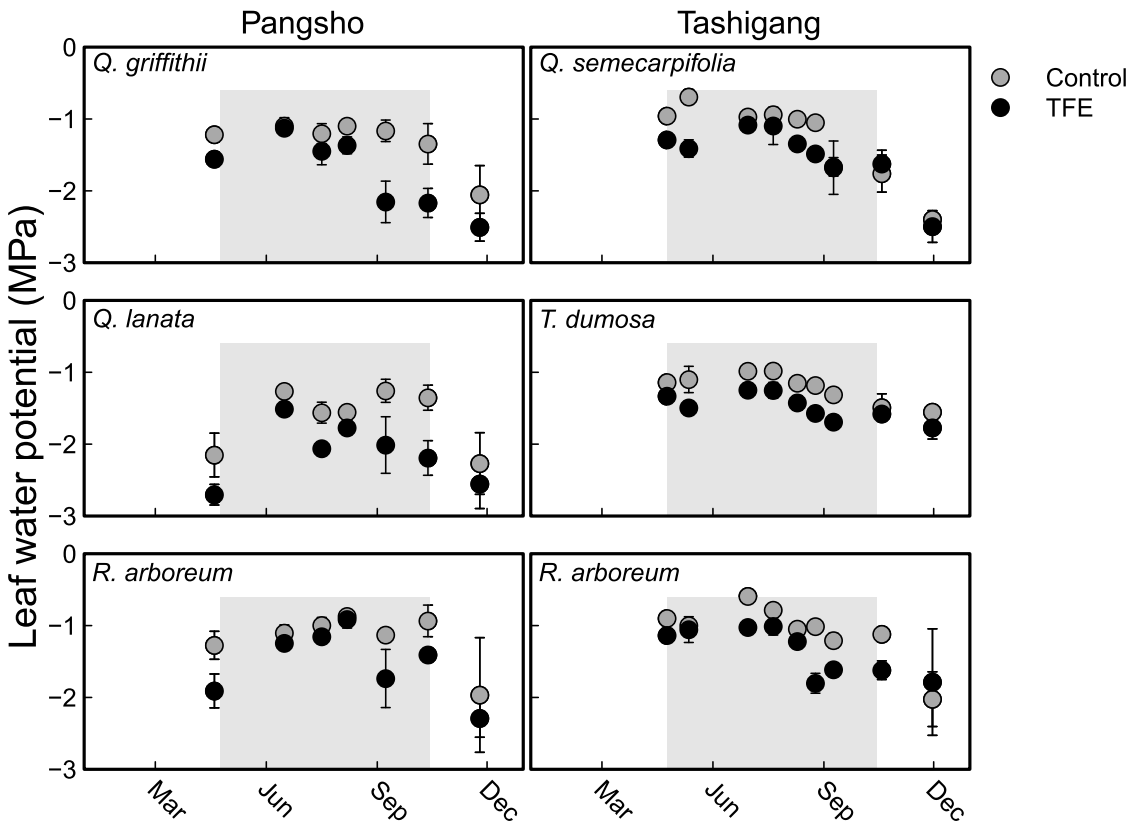

Fig. 1. Leaf water potential in a broadleaved (Pangsho, 2.640 m a.s.l.) and a coniferous mixed (Tashigang, 3.260 m a.s.l.) forest in the Eastern Himalayas, Bhutan in 2015. Shown are daily mean values of trees in control and throughfall exclusion (TFE) treatments separately for dominating tree species and understory trees (*R. arboreum*). Error bars indicate standard error of the mean. gray rectangles represent the time were TFE treatments (roofs) were present.

down to −2.0 MPa, respectively. In Pangsho forest, a slightly larger decrease in Ψ was observed for *Quercus* species than for *R. arboreum*. However, treatment effects did not differ significantly between tree species at both sites, as assessed by two-way ANOVA (Interaction term TFE x species $p < 0.05$).

3.3. Tree stem growth, tree mortality, and litterfall

Tree mortality was not observed at any treatment plot during the whole study period. In Pangsho forest, stem diameter increment for both dominant tree species *Q. lanata* and *Q. griffithii* were similar in the second year and lower in third year of roof installations when comparing TFE to control plots. In Tashigang forest, in contrast, the diameter increment was lower in the second and third year after TFE installation for both dominant tree species, *T. dumosa* and *Q. semecarpifolia*. Due to the high variability among diameter increment rates of individual stems (Table 2), the differences in stem diameter increment between TFE and control were, however, statistically not significant at both sites (p>0.05).

Table 2
Average stem diameter increment (mm) derived from dendrometer measurements (42 trees equipped with dendrometers) in Pangsho forest (upper panel) and Tashigang forest (lower panel) for 2015 and 2016. Given are mean values ± standard deviation for control and throughfall exclusion (TFE) plots.

Site	Tree species	Year	
Pangsho		2014–2015	2015–2016
Control	*Quercus lanata*	2.9 ± 2.7	3.1 ± 3.67
	Quercus griffithii	3.3 ± 2.8	4.0 ± 3.9
TFE	*Quercus lanata*	3.0 ± 3.0	2.0 ± 2.0
	Quercus griffithii	3.6 ± 1.5	2.6 ± 3.5
Tashigang			
Control	*Tsuga dumosa*	4.8 ± 3.4	7.1 ± 3.4
	Quercus semecarpifolia	0.8 ± 2.8	1.4 ± 0.3
TFE	*Tsuga dumosa*	2.6 ± 3.4	2.8 ± 3.2
	Quercus semecarpifolia	0.7 ± 0.3	0.7 ± 0.2

Above ground litterfall was unaffected by TFE at both sites during the second TFE treatment year 2015, but was about 10% higher at the lower elevation deciduous site at Pangsho (control: 677 ± 83 g m^{-2}, TFE: 674 ± 128 g m^{-2}) when compared to the higher elevation conifer dominated site at Tashigang (control: 613 ± 120 g m^{-2}, TFE: 596 ± 282 g m^{-2}). In 2016 a number of the litter traps were damaged by animals, thus preventing a thorough determination of annual litter input or TFE effects.

3.4. Fine root biomass and necromass

The standing fine root biomass to 30 cm soil depth was lower at Tashigang (378 g m^{-2} dry root biomass equivalent to 196 g C m^{-2}) compared to Pangsho forest (593 g m^{-2} biomass equivalent to 304 g C m^{-2}) for the summed values of all measuring times. There were clear differences between the two sites in the root biomass distribution down the soil profile. In the mixed coniferous-dominated forest at Tashigang, between 40 and 57% of the total (0–30 cm) fine root biomass was located in the top 0–10 cm layer, whereas in the oak forest at Pangsho, between 57 and 62% of the total fine root biomass was located in the top 0–10 cm.

At Pangsho forest fine root biomass was unaffected during the first TFE year. In the second year, fine root biomass in TFE decreased in the 0–10 cm soil depth layer, but it was not affected in deeper soil horizons, as indicated by a significant interaction between TFE treatment and soil depth (Fig. 2a). At Tashigang forest, during 2014 and 2015, TFE had no significant effect on fine root biomass stocks in any soil depth layer (Fig. 2b).

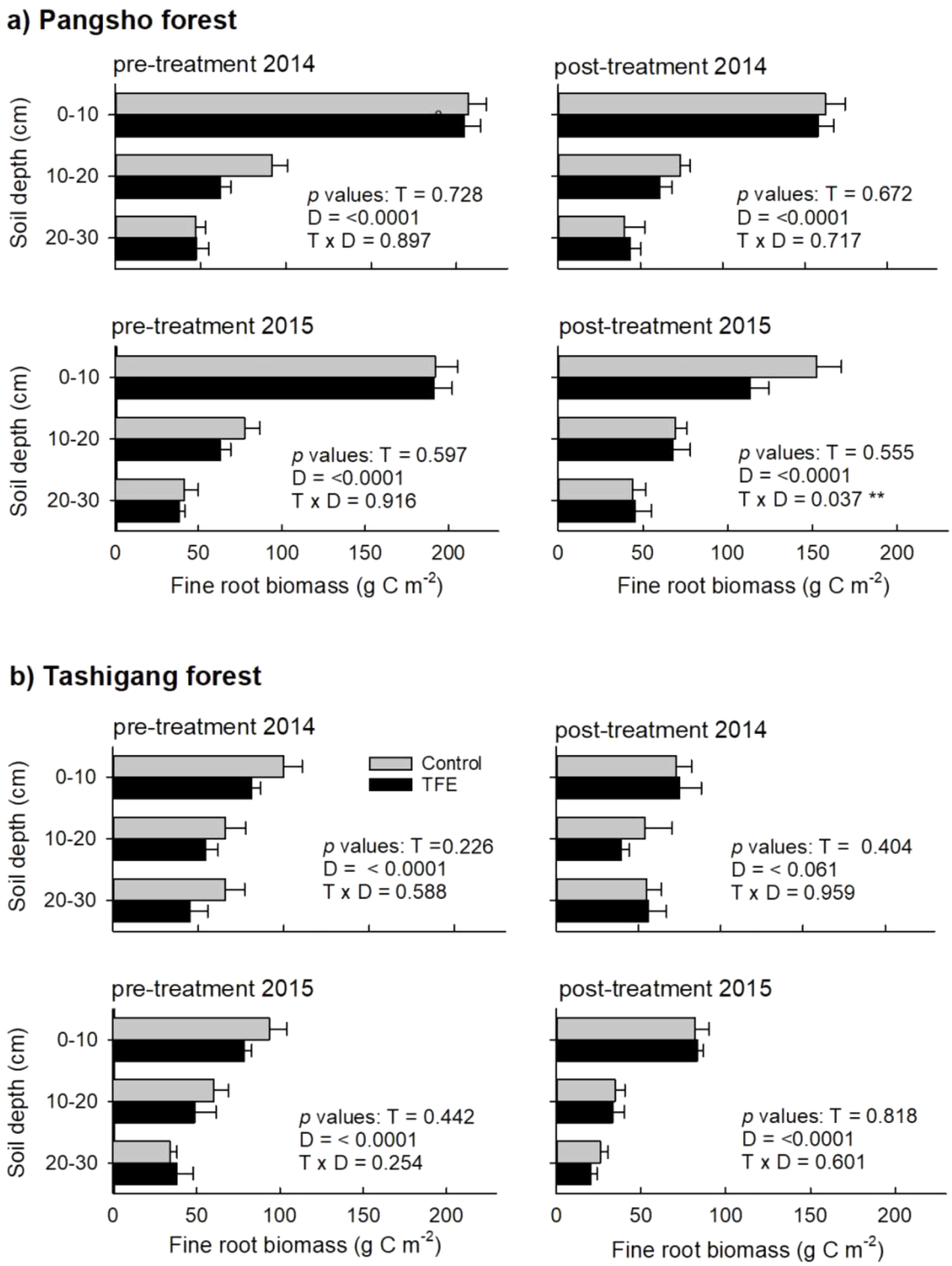

Fig. 2. Fine root biomass C at the (a) broadleaved Pangsho forest site (2.640 m a.s.l.) and (b) the conifer dominated mixed forest site at Tashigang (3.260 m a.s.l.). Living fine root C stocks at three soil depth layers in control (gray) and throughfall exclusion (TFE, black) plots. Pre-treatment assessments were completed each study year before applying the rain-out shelters; post-treatment assessments were conducted shortly after dismounting the roofs. Given are the test statistics that were used to analyze the effect of TFE (treatment, T), soil depth (D) and their interaction ($T \times D$).

Fine root necromass (Fig. 3) at both sites was on average 13–27% of the living fine root biomass. At the oak dominated forest at Pangsho, TFE resulted in a significant increase in fine root necromass in both treatment years (Fig. 3), while there was no difference between control and TFE at the conifer dominated Tashigang forest (Fig. 3).

3.5. *Fine root production and turnover*

Fine root production in total ingrowth cores down to 30 cm soil depth was greater at Pangsho forest than at Tashigang forest (Fig. 4) and was significantly increased after TFE. At Pangsho forest, fine root production was doubled by the TFE treatment. No fine root necromass was

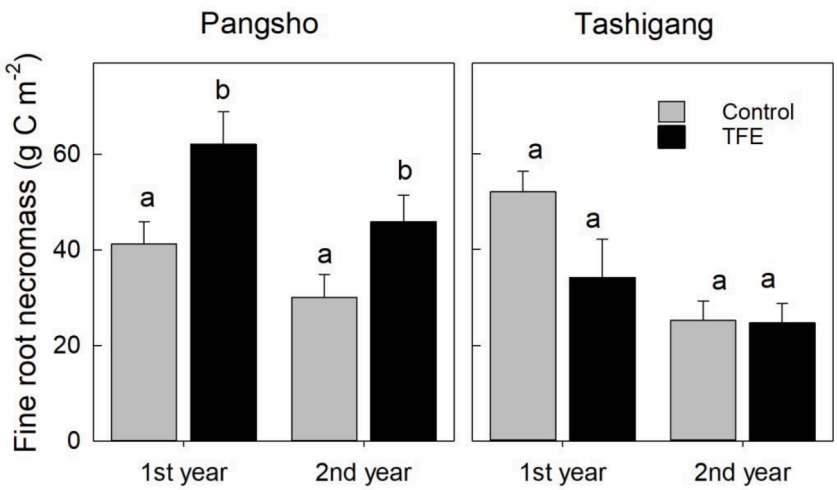

Fig. 3. Fine root necromass C in a broadleaved (Pangsho, 2.640 m a.s.l.) and a conifer dominated mixed (Tashihgang, 3.260 m a.s.l.) forests during 2014 (1st year) and 2015 (2nd year). Shown are mean values ($n = 10$) of control and throughfall exclusion (TFE) treatments. Error bars indicate the standard error of the mean. Different letters indicate statistically significantly differences ($p > 0.05$).

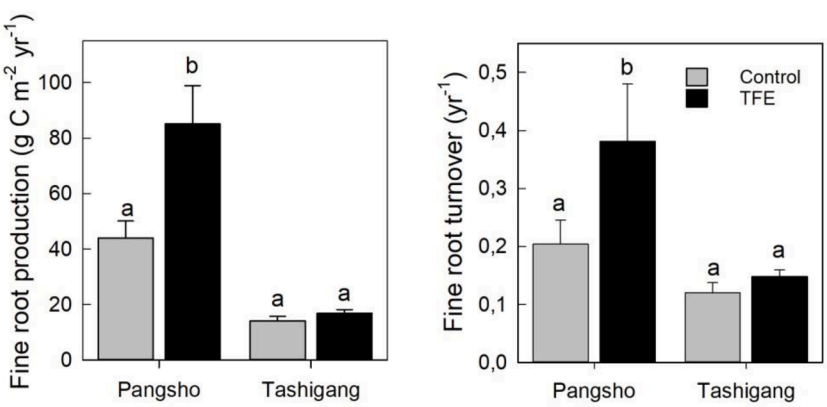

Fig. 4. Fine root production (left) and turnover (right) in a broadleaved (Pangsho, 2.640 m a.s.l.) and a conifer dominated mixed (Tashihgang, 3.260 m a.s.l.) forest in the Eastern Himalayas, Bhutan. Shown are mean values ($n = 10$) of control and throughfall exclusion (TFE) treatments. Error bars indicate standard error of the mean. Fine root production refers to a period of 12 months root ingrowth into root free ingrowth-cores. Fine root turnover rate was estimated as ratio of fine root production and standing fine root biomass. Different letters indicate statistically significantly differences ($p > 0.05$).

found in the ingrowth cores. The fine root production (Fig. 4) was low when compared to the standing fine root biomass, and consequently, low rates of fine root turnover were determined (Fig. 4). At Pangsho forest, TFE resulted in a significant ($p = 0.042$) increase in fine root turnover, but no effect was shown at Tashigang forest.

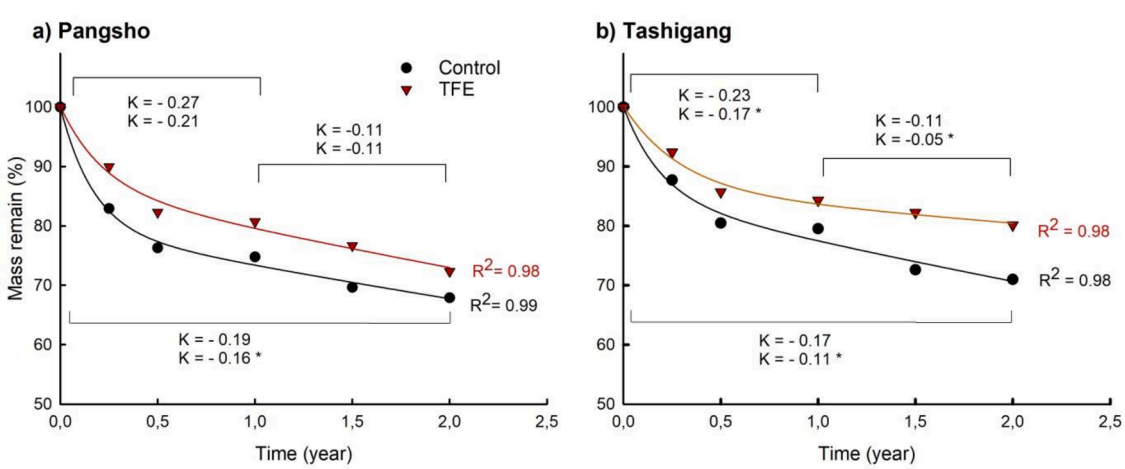

Fig. 5. Decay curves of *T. dumosa* fine roots in a conifer dominated mixed forest (Tashigang, 3.260 m a.s.l.) (a) and *Q. lanata* fine roots in a broadleaved forest (Pangsho, 2.640 m a.s.l.) (b) in the Eastern Himalayas, Bhutan. Cumulative mass remaining data (mean, $n = 8$) after five time-intervals during two years of litterbag incubation. Decay constants (K) are shown for the whole 24 months, the first year, and for mass loss during months 12–24. Stars indicate significant differences ($p < 0.05$).

3.6. Fine root decomposition

Throughfall exclusion significantly decreased fine root mass losses at both sites (p = 0.001 and 0.012) during the whole 24 months root litterbag incubation (Fig. 5). At the end of the incubation period, mass loss from fine root in control and TFE plots was 32±0.69 and 28±1.40% in Pangsho, and 29±0.61 and 20±0.88% in Tashigang, respectively. While the TFE effect on root litter mass loss was significant at both forest sites during the initial 12 months, there was no TFE effect from months 12 until months 24 at the Pangsho forest site. At the Tashigang forest, fine root litter mass loss was consistently reduced throughout the whole incubation period (Fig. 5)

3.7. Soil CO_2 efflux

At the Pangsho forest, daily mean Rs rates ranged from 1.39 to 11.52 and from 0.96 to 6.34 μmol m^{-2} s^{-1} in control and TFE treatments, respectively (Fig. 6a). At Tashigang forest daily mean R_S rates ranged from 1.25 to 7.62 and from 0.56 to 5.46 μmol m^{-2} s^{-1} in control and TFE treatments respectively (Fig. 6b). The generally higher soil CO_2 effluxes at all plots during the first year (Fig. 6) are a methodological artefact because base collars for the soil respiration chamber had not yet been installed until spring 2015. Seasonal patterns in Rs clearly followed the course of soil temperature at both sites and treatments. Soil temperature alone explained 89% of the temporal variability in Rs (Table S1). The constantly low soil moisture in TFE treatments throughout the study (Fig. 6e, F) explains why no temporal soil moisture effects on Rs could be determined by the model, and why soil temperature was the dominant predictive variable in the TFE treatment as well.

Soil CO_2 efflux was significantly lower in TFE treatments at both sites (Table S2). Annual estimates for Rs are shown in Fig. 7. In 2015 (second study year), TFE decreased annual efflux CO_2 by 39 and 58% at the Pangsho and Tashigang forest, respectively. In 2016 (third study year), TFE decreased annual efflux CO_2 by 46 and 63% at the Pangsho and Tashigang forest, respectively. Soil CO_2 efflux at TFE plots of both forests recovered within days after re-wetting to levels close to those of control plot fluxes after roof removal in the first treatment year 2014 (Fig. 6a, 6b). In the second and third treatment year, soil CO_2 effluxes recovered as well after roof removal at Pangsho forest, but fluxes remained at generally lower levels because roofs were dismounted only during the dormant seasons (Fig. 6a). At Tashigang forest, soil moisture showed a generally declining trend at the TFE plots throughout the three treatment years and became increasingly limited during roof-free periods as well (Fig. 6f, Table S2). In accordance, soil CO_2 efflux at TFE plots did not fully recover after roof-removal and remained below those of control plots during the (roof-free) dormant season 2015/16.

4. Discussion

4.1. Above ground responses

Throughfall exclusion significantly reduced mid-day leaf water potentials of the overstorey trees in both forests. The oak dominated lower-elevation Pangsho forest responded more strongly and leaf water

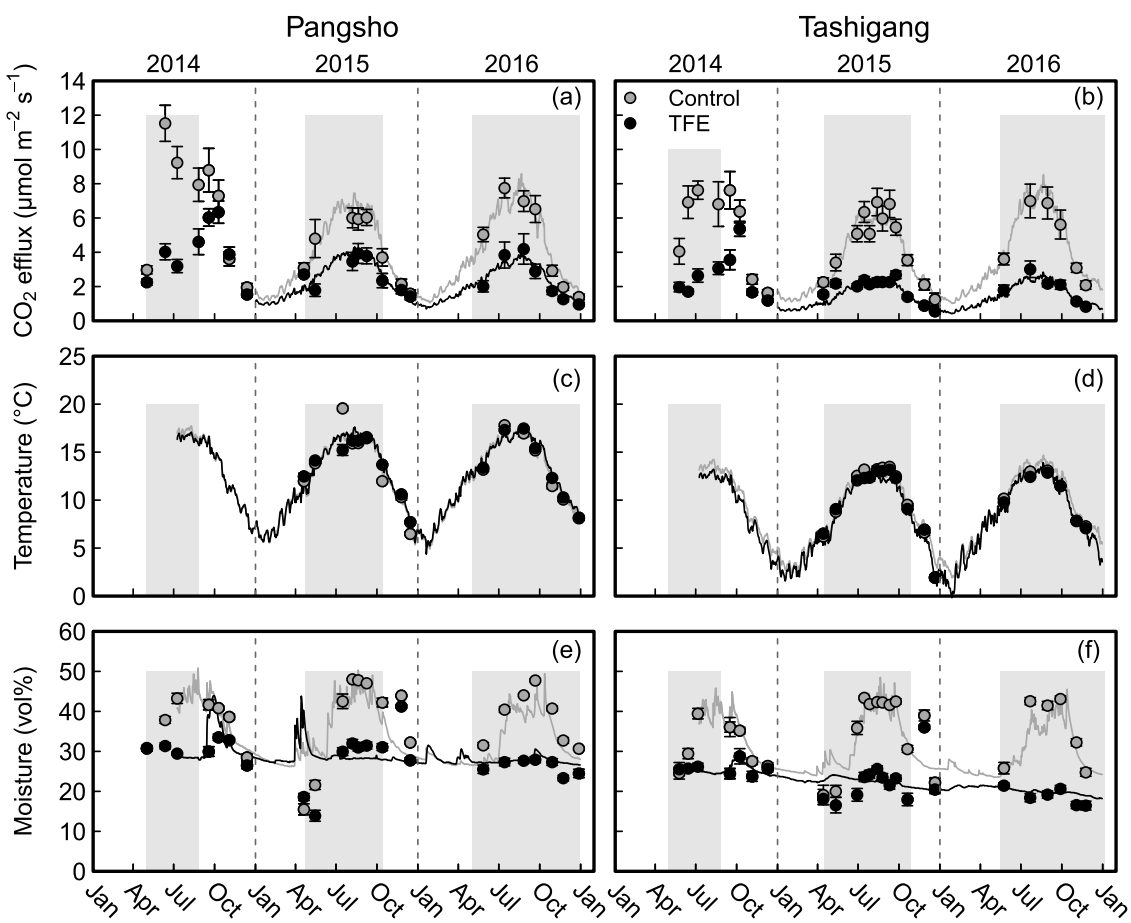

Fig. 6. Seasonal course of soil CO_2 efflux (a, b), soil temperature (c,d), and soil moisture (e,f) in a broadleaved (Pangsho, 2.640 m a.s.l.) and a conifer dominated mixed (Tashigang, 3.260 m a.s.l.) forest in the Eastern Himalayas, Bhutan from 2014 until 2016. Shown are daily mean values (n = 10) of control and throughfall exclusion (TFE) treatments. Error bars indicate standard error of the mean. Solid lines represent daily mean values of modelled soil CO_2 efflux rates and continuously measured soil temperature and soil moisture values. Shaded areas represent the time were TFE treatments (roofs) were present.

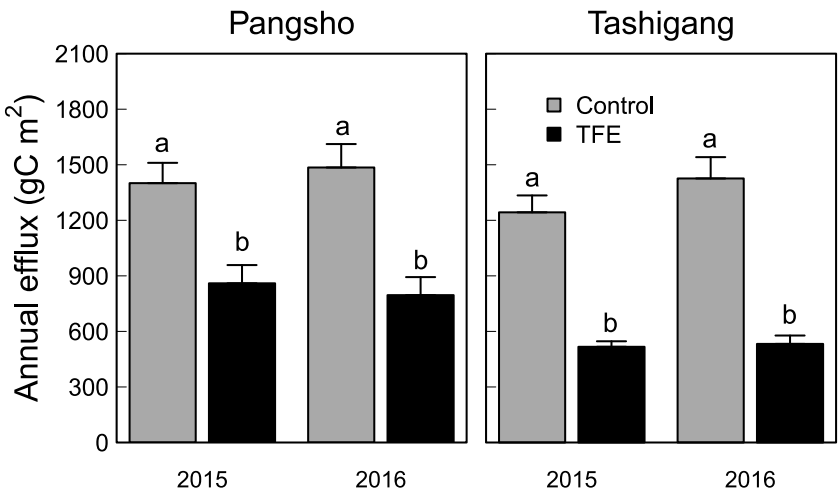

Fig. 7. Total annual soil CO_2 efflux in control and throughfall exclusion (TFE) treatments in broadleaved (Pangsho) and conifer dominated mixed (Tashigang) forests in the Eastern Himalayas, Bhutan in 2015 and 2016. Given are mean values and standard error of the mean ($n = 10$). Different letters indicated significant ($p < 0.05$) differences between treatments. Efflux rates were predicted by means of linear mixed effects models.

potentials were already lower before roof installations in the second treatment year 2015 (Fig. 1). This suggests the trees were still affected from TFE in the first year of the study. Unexpectedly, leaf water potentials in control, as well as in TFE plots increased during the early TFE phase (Fig. 1) though they were expected to decrease under TFE. An explanation for the increase could be a generally higher air humidity and hence lower vapor pressure deficit after the onset of the monsoon season. During the latter phase of TFE, however, leaf water potentials of both *Quercus* species dropped below −2 MPa at Pangsho forest, while the decrease was less pronounced for the understory species *R. arboreum.* This finding corresponds to an earlier study on Himalayan tree species (Poudyal et al., 2004).The comparatively minor decrease in leaf water potentials at the higher-elevation coniferous dominated Tashigang forest suggests that TFE imposed only a moderate physiological response to reduced water availability at this site. The reasons why leaf water potentials at Pangsho responded more sensitively to TFE may most likely lay in site specific climatic preconditions but might also be related to wood and leaf anatomy of the tree species growing at the different sites. For instance, ring porous *Q. griffithii* has the largest vessel diameter (252 μm) of all Indian oaks, whereas diffuse porous *Q. semecarpifolie* has the smallest vessel diameters (100 μm) (Gupta and Gupta, 2020). This could explain the stronger TFE effect on water potentials of *Q. griffithii,* when compared to *Q. semecarpifolie* (Klein, 2014). Soils at both forest sites showed similar features with regard to depth (> 1 m), clay mineralogy and organic matter contents (Wangdi et al., 2017). Hence, the soil water holding capacity can be considered as similar. However, Tashigang forest receives a ~15% higher annual rainfall and lower air temperatures impose a shorter growing season. Hence, the water demand of the vegetation and the associated soil water losses start later in the year at the higher-elevation Tashigang forest. This could also be a reason why soil moisture in deeper soil layers was less reduced by TFE at Tashigang, when compared to Pangsho (Wangdi et al., 2017). Another reason for the weak response of leaf water potentials to TFE may be lower vapor pressure deficits at the higher altitude site that is frequently covered in fog and clouds during the monsoon periods (0.190 kPa at Tashigang and 0.213 kPa at Pangsho). Particularly the high incidence of fog could drive foliar water uptake by trees, particularly at low vapor pressure deficits (Berry et al., 2019). In a recent review, Schreel & Steppe (2020) list species capable of foliar water uptake in different climates and propose that 100% of the studied 33 tree species in monsoon climates were capable of leaf water uptake.

Although the lower leaf water potentials indicate a physiological response to the reduced water availability, no tree mortality was observed during the three study years at any of the treatment plots. This highlights that measured leaf water potentials were still above the levels where significant water transport failure and xylem embolisms due to severe drought stress would be expected (Skelton et al., 2021). In accordance, we did not observe any leaf shedding or other visual signs of drought in the tree crowns at both forest sites.

Against our expectations (H1), radial stem increment growth remained largely unaffected by TFE until the second treatment year (2015), particularly at Pangsho forest. However, during the third year (2016), diameter increment measurements indicate 35% lower stem growth of both *Quercus* species at Pangsho forest TFE plots and 61 and 52% lower stem growth of *T. dumosa* and *Q. semecarpifolia* at Tashigang forest TFE plots, respectively (Table 2). Since increment growth measurements started in 2015, we can only speculate about the initial, first TFE season (2014) growth response. Since growth was rather unaffected by TFE in 2015, it is, however, likely that growth was also unaffected in 2014, the first TFE year with the shortest and least severe throughfall reduction. Lagged responses of trees to drought have been observed frequently, e.g. for oaks (Becker et al., 1995; Vanhellemont et al., 2019; Vanoni et al., 2016) or Scots pine (Bigler et al., 2006; Galiano et al., 2011) but not for a number of other conifer species (Song et al., 2021). The two years of lagged growth response suggest that it takes a relatively long lead-in time until the water shortage manifests in reduced stem growth, confirming a general global trend that forest above ground net biomass productivity is more negatively affected during longer-term drought than during short-term drought (Gao et al., 2019). Mature trees typically contain significant C reserves in form of nonstructural C compounds, which could have been mobilized to sustain tree stem growth during the first two TFE years (Piper and Paula, 2020). Another reason for the lagged growth response could be the different springtime precipitation and soil moisture patterns during the individual years. In 2015, a significant amount of precipitation fell before roof closure and increased soil moisture in all plots accordingly (Fig. 6). In 2016, much less precipitation fell prior to roof-installations, hence imposing dry conditions during springtime already. It has been shown that springtime water supply is highly correlated to annual radial stem increment growth in the Himalaya region (Dawadi et al., 2013; Gaire et al., 2017; Panthi et al., 2017). Hence not only the magnitude, but also the timing of precipitation likely plays a crucial role in the aboveground stem/biomass growth response.

The stem diameter increment was more reduced at Tashigang forest than at the lower-elevation mixed oak forest at Pangsho, although leaf water potentials were less affected by TFE. This could point towards a generally higher sensitivity of *T. dumosa* to dry soil conditions. Lower drought tolerance of Tsuga species was found by DeClerck et al. (2006)

and Song et al. (2021). In a dendrochronological analysis, *T. dumosa* in Tibet showed also a strong negative growth response to higher air temperatures (Fan et al., 2008).

The present study allowed for an assessment of sequential three year of TFE effects on tree mortality and stem growth but it has to be kept in mind that the different studied tree species could show lagged drought responses long after precipitation returns to average precipitation levels (Martin-StPaul et al., 2013; Trugman et al., 2018). An assessment of such potential post-drought effects, however, was beyond the scope of this current study and is recognized as an important issue regarding further research at the sites.

Some caveats of the throughfall manipulation method must be considered when interpreting the above ground responses to TFE. Simulating drought on an ecosystem scale is difficult in a mature forest, and ground roofs can only incompletely resemble the full extent of a natural drought. While the throughfall exclusion to the soil surface might realistically mimic the impact on soil processes, the application of ground roofs does not impact air humidity and air vapor pressure deficits in the tree crown space (Leuzinger et al., 2015). Evaporation can therefore be expected to be significantly lower under TFE than during natural dry spells (McGregor et al., 2021; Oishi et al., 2010). Even foliar water uptake (Limm et al., 2009; Schreel and Steppe, 2020) might have occurred during TFE, as foggy conditions often prevail along the mountain slopes during the monsoon season, and may have attenuated the TFE effect. Plant water demand and hence water uptake are therefore likely lower under the artificial TFE treatments than during natural drought periods (Ding et al., 2021). Accordingly, particularly the above ground ecosystem responses to drought could have been underestimated by the applied TFE method and could be more pronounced during natural dry spells, but even the TFE effect size on soil moisture could indirectly be lessened by these methodological caveats. Nevertheless, air temperature and precipitation throughout the study period were comparable to long-term records, suggesting above ground ecosystem responses to TFE were not biased by climate anomalies, such as naturally occurring drought or exceptionally wet periods.

4.2. Fine root responses

Overall, fine root biomass stocks at the two study sites (593 g m^{-2} at Pangsho and 378 g m^{-2} at Tashigang) corresponded to those observed at other studies within the Himalaya region. In a previous study, (Upadhyay et al., 2003) reported fine root biomass stocks of 537 g m^{-2} and 267 g m^{-2} in the top 30 cm soil depth in Central Himalayan evergreen oak (*Quercus floribunda*) and subtropical pine (*Pinus roxburghii*) forests respectively. Joshi & Garkoti (2021) estimated fine root biomass stocks of about 300 to 450 g m^{-2} in the top 30 cm mineral soil in *Q. leucotrichophora* forests and mixed forests of *Q. leucotrichophora* and *A. nepalensis* forest in Central Himalayan India. About 40 to 50% of the fine roots occurred in the top 0–10 cm soil layer, which is in accordance with the topsoil contribution of 44% in the mixed oak forest at Pangsho in our study.

The fine root responses to TFE differed substantially between Tashigang and Pangsho forests. Fine root biomass and necromass, fine root production, as well as fine root turnover remained unaffected by TFE at Tashigang forest. This contradicted our hypotheses (H2) and indicates that tree fine roots at the higher elevation, conifer dominated Tashigang forest are highly resistant to topsoil drying. The drastically reduced soil CO_2 efflux may, however, point towards a reduced physiological activity of the fine roots present. An explanation for the overall lack of response of the measured fine root parameters to severe topsoil drying could be water redistribution from deeper growing taproots to the fine roots in the topsoil (Burgess et al., 1998). Further, we cannot exclude that tree species specific fine root responses to TFE, might have affected and changed the species specific fine root contribution to the measured bulk root biomass (Zwetsloot and Bauerle, 2021). *Tsuga* species, which were among the dominant trees at Tashigang forest are generally more shallow rooted (Minore, 1983) when compared to the co-dominating *Q. semecarpifolia* and *A. densa* trees (Meinzer et al., 2007). Hence, it cannot be excluded that e.g. *Q. semecarpifolia* and *A. densa* fine root biomasses increased in abundance on the expense of *T. dumosa*; but this remains speculative and merits further investigation. Fine root decomposition at Tashigang was suppressed by TFE during both years, but this was not reflected in the root necromass pool. However, fine root litter bags were only applied in the very topsoil, whereas the measured necromass is an average of the whole 0–30 cm profile. Root litter decomposition within the 10–30 cm soil layer could therefore have masked the effects on the whole 0–30 cm profile necromass dynamics. However, suppressed fine root decomposition during both study years matches well with the sharply reduced soil CO_2 efflux rates during the same period.

At Pangsho forest, fine roots showed a more differentiated response pattern. Although also here there was no TFE effect on fine root biomass during the first year, fine root biomass in the topsoil (0–10 cm) was reduced during the second TFE season, indicating first root biomass responses to drought stress. Fine root necromass was significantly enhanced during both years, suggesting that topsoil drought led to increased fine root mortality (Leonova et al., 2022; Moser et al., 2014). On the other hand, significantly increased root in-growth suggests that fine root production was simultaneously stimulated by TFE, resulting in an overall faster fine root turnover in the dry topsoil. Higher fine root production would represent a reasonable plant C allocation strategy to compensate for mortality and expand, and/or maintain, nutrient and water forage (Bloom et al., 1985; Gaul et al., 2008). Like Tashigang, root decomposition rates were suppressed by TFE at Pangsho forest. However, the effect was not as pronounced as at Tashigang and lasted only during the first 12 months after burying the litter bags. A stronger response might be related to a continuing decrease in soil moisture at Tashigang TFE during the second and third study year and rather stable moisture conditions at Pangsho TFE during that period (Fig. 6c). This pattern is consistent with an overall less pronounced soil CO_2 efflux reduction at Pangsho forest TFE plots, when compared to TFE plots at Tashigang forest.

4.3. Soil CO_2 efflux

Carbon dioxide emissions from the untreated soils were in a similar range at both study sites, but were in the upper range of temperate forest ecosystems in similar climates (Jian et al., 2021). Although of considerable magnitude, they, however, still were lower than those of a low-elevation young pine plantation in the Western Himalayas (Singh and Parida, 2019).

Soil CO_2 efflux at both sites sharply declined under TFE, and thus confirmed our hypothesis (H3), that drought will decrease the activity of decomposer microbes and hence their respiration rates. The reduction in soil CO_2 efflux was more pronounced at Tashigang forest than at Pangsho, which was paralleled by a more distinct and continuing decrease in soil moisture. Generally, the sharp decline could, at least partially, have resulted from a lowered rhizosphere respiration. However, the actual TFE effects on the heterotrophic and autotrophic flux components could not be distinguished in this study. The decrease in soil CO_2 efflux was more pronounced at Tashigang forest, where fluxes decreased by almost two-thirds under TFE. Such a severe effect has yet been rarely observed in throughfall exclusion experiments in temperate forests. The 40–50% reduction in soil CO_2 efflux at Pangsho forest is within the range of observations from similar TFE experiments in other forests ecosystems e.g. (Borken et al., 2006; Schindlbacher et al., 2012; van Straaten et al., 2011). We did not observe any extraordinary peaks in soil CO_2 after soil rewetting ("Birch effect"; (Jarvis et al., 2007)) after the roofs were removed in autumn. Only in the first study year soil CO_2 efflux increased slightly after roof deinstallation, likely due to an increase in soil moisture. Except of that, soil CO_2 fluxes tended to be lower even during the autumn and spring periods when the roofs were dismounted;

particularly during the later treatment years 2015 and 2016 (Fig. 6). At Tashigang forest, soil CO_2 efflux only recovered to control levels during autumn after roof removal in the first treatment year 2014. Afterwards soil CO_2 efflux steadily remained below TFE plots levels, no matter if roofs were applied or not. As fine root biomass was barely affected by TFE, such a general down-regulation of respiratory fluxes suggests that the microbial community was significantly and persistently affected by the drought treatment. If TFE resulted in lower microbial biomass, changes in the community composition or in the microbial C use efficiency, was not assessed in detail in this study. However, such persistent effects of TFE or natural drought on soil CO_2 efflux beyond rewetting have also been observed in other forests (Schindlbacher et al., 2012). This may indicate that the decomposition of soil organic matter is negatively affected beyond the actual drought situation. Increasing water repellency of organic matter with increasing drought duration can be another important mechanism within this regard (Goebel et al., 2011; Sánchez-García et al., 2020). If and how soil CO_2 efflux recovers on the longer-run remains yet open for the two study sites which still (2020) undergo TFE treatment.

4.4. Ecosystem carbon

Although several important ecosystem C fluxes have been measured and/or estimated in the two forests, estimating the effects of TFE on the overall ecosystem C budget remains challenging. The three years soil CO_2 efflux record, for instance, allowed for a precise assessment of TFE effects on total soil respiration, but the detailed TFE effects on the heterotrophic and autotrophic respiration keep an open question. It might be noted that we applied a root-exclusion approach at all sites to differentiate between autotrophic and heterotrophic soil CO_2 efflux. However, this approach failed at both forest sites, as CO_2 fluxes from root-exclusion plots remained mostly at, or even above, fluxes from control plots. Additional CO_2 from decomposing fine roots or soil moisture differences between treatments may have been the cause (Díaz-Pinés et al., 2010); but it was beyond our capacity to determine this in the present study. Nevertheless, Wangdi et al. (2017) estimated autotrophic respiration in the untreated control plots using laboratory incubations and modeling, and report autotrophic contributions to the total soil CO_2 efflux from close to zero during winter to around 40–50% during summer. Hence, about 60% of the annual CO_2–C efflux was attributed to soil C loss from the untreated forest soils. Assuming autotrophic-heterotrophic flux ratios hold true for TFE too, topsoil-drying may have resulted in strong reduction of gaseous soil C losses by $\sim$ 4 t C ha^{-1} yr^{-1} at Pangsho, and $\sim$ 6 t C ha^{-1} yr^{-1} at Tashigang forest during 2015 (second TFE year).

Another important belowground C flux is the input of root carbon into the soil pool. Though fine root biomass stocks were not or only slightly affected, root ingrowth suggests higher fine root production and turnover at Pangso forest under TFE. Accordingly, fine root C input into the topsoil had increased at the oak dominated Pangsho forest by $\sim$ 0.4 t C ha^{-1} yr^{-1} during 2015. This however is a rough estimate and holds considerable uncertainty related to the potential caveats of the root ingrowth method (Oliveira et al., 2000). Another, potentially important C flux with regard of soil C formation is root exudation into the rhizosphere (Sokol et al., 2019). This C flux was not measured and TFE effects remains unclear, but could be relevant with regard to the overall plant-soil response to drought (Williams and de Vries, 2020). Brunn et al. (2022) for instance suggested fine root C exudation of about $\sim$350 kg ha^{-1} y^{-1} in a mixed temperate forest and found that exudation was maintained or even increased during drought periods.

With more than 3 t C ha^{-1} yr^{-1} at both sites, above ground litter input was a major C flux from the plants to the soil. Above ground litter input to the forest soil was unaffected in the second TFE year, the only year with sufficient above ground litterfall data. It would have been of great interest to know how aboveground litterfall was affected in the third TFE year 2016, during which tree growth showed first TFE responses. However, as several litter traps were destroyed by bears, and due to a poorly documented change in the litter drying procedure, the 2016 data were not reliable enough to be included in our analyses. Nonetheless, we visually did not observe any litter shedding or litter accumulation during 2016.

Although delayed by two years, TFE manifested in reduced tree growth as assessed by diameter increment measurements. Thus, it is plausible to speculate that a decrease in plant C uptake was to a certain degree outbalanced by the TFE induced reductions in ecosystem C losses. We hence conclude that longer lasting drought periods, which lead to severe topsoil drying, could, in contrast to our initial expectations led to an, at least temporary, stable ecosystem C balance in this high elevation forest ecosystems. If such a net ecosystem C pseudo-equilibrium, which is primarily related to decreased decomposition of topsoil organic carbon and an increased root C input into the soil, is durable or not, depends on how decomposer microbes will respond to longer-term rewetting. Although soil C may accumulate during drought (Brunn et al., 2023), it might become overall less stable and susceptible to decomposition once annual precipitation inputs again reach normal levels (Yang et al., 2021). Also longer-term lag-effects on tree physiology and tree health remain open, but could significantly affect ecosystem C dynamics after the actual drought, e.g. if tree mortality increases post-drought. All this warrants further longer-term investigations, which are currently undergoing at the two forest sites.

Declaration of Competing Interest

The authors declare that they have no known competing financial interests or personal relationships that could have appeared to influence the work reported in this paper.

Data availability

Data will be made available on request.

Acknowledgement

We are highly grateful to all the staff of Renewable Natural Resources Research and Development Centre, Yusipang for all the support for the field work. We also thank, the management and staff of the Ugyen Wangchuck Institute for Forestry Research and Training, Bumthang, for providing additional support for the study. This study was part of the work package I of the mega roofing project. The whole project was supported by the BC–CAP project (Climate Change Adaptation potentials of forests in Bhutan –Building human capacities and knowledge base) jointly implemented by the Department of Forest and Park Services, Bhutan and University of Natural Resources and Applied Life Sciences (BOKU), Austria with funding from Government of Austria, through the Ministry of Agriculture, Forestry, Environment and Water Management. DLG was also supported by the Ministry of Education, Youth and Sports within the National Sustainability Program NPU I, grant No. LO1415. MM has received support from an Erwin Schrödinger Fellowship from the Austrian Science Fund (FWF project number J-4369) and from a personal research grant from the ETH Board awarded to Prof. Andreas Rigling.

Supplementary materials

Supplementary material associated with this article can be found, in the online version, at doi:10.1016/j.agrformet.2023.109471.

References

Aadhar, S., Mishra, V., 2021. On the occurrence of the worst drought in South Asia in the observed and future climate. Environ. Res. Lett. 16 (2), 024050 https://doi.org/10.1088/1748-9326/abd6a6.

Adams, H.D., Zeppel, M.J.B., Anderegg, W.R.L., Hartmann, H., Landhäusser, S.M., Tissue, D.T., Huxman, T.E., Hudson, P.J., Franz, T.E., Allen, C.D., Anderegg, L.D.L., Barron-Gafford, G.A., Beerling, D.J., Breshears, D.D., Brodribb, T.J., Bugmann, H., Cobb, R.C., Collins, A.D., Dickman, L.T., McDowell, N.G., 2017. A multi-species synthesis of physiological mechanisms in drought-induced tree mortality. Nature Ecol. Evol. 1 (9), 1285–1291. https://doi.org/10.1038/s41559-017-0248-x.

Arend, M., Link, R.M., Patthey, R., Hoch, G., Schuldt, B., Kahmen, A., 2021. Rapid hydraulic collapse as cause of drought-induced mortality in conifers. Proc. Natl. Acad. Sci. 118 (16).

Barton, K., 2018. Package MuMIn: multi-model inference. R package version 1.42. 1.

Becker, M., Bert, G., Bouchon, J., Dupouey, J.-.L., Picard, J., Ulrich, E., 1995. Long-term changes in forest productivity in northeastern France: the dendroecological approach. Forest Decline and Atmospheric Deposition Effects in the French Mountains. Springer, pp. 143–156.

Berry, Z.C., Emery, N.C., Gotsch, S.G., Goldsmith, G.R., 2019. Foliar water uptake: processes, pathways, and integration into plant water budgets. Plant Cell Environ. 42 (2), 410–423.

Bigler, C., Bräker, O.U., Bugmann, H., Dobbertin, M., & Rigling, A. (2006). Drought as an inciting mortality factor in Scots pine stands of the Valais, Switzerland. *Ecosystems*, 9 (3), 330–343.

Bloom, A.J., Chapin III, F.S., Mooney, H.A, 1985. Resource limitation in plants-an economic analogy. Annu. Rev. Ecol. Syst. 16 (1), 363–392.

Borken, W., Davidson, E.A., Savage, K., Gaudinski, J., Trumbore, S.E., 2003. Drying and wetting effects on CO2 release from organic horizons. Soil Sci. Soc. Am. J. 67, 1888–1897.

Borken, W., Savage, K., Davidson, E.A., Trumbore, S.E., 2006. Effects of experimental drought on soil respiration and radiocarbon efflux from a temperate forest soil. Glob. Chang Biol. 12, 177–193.

Bouskill, N.J., Lim, H.C., Borglin, S., Salve, R., Wood, T.E., Silver, W.L., Brodie, E.L., 2013. Pre-exposure to drought increases the resistance of tropical forest soil bacterial communities to extended drought. ISME J. 7 (2), 384–394.

Bouyer, L., Vincent-Barbaroux, C., Le Jan, I., Delaunay, A., Marchand, L., Feinard-Duranceau, M., Sallé, A., Chassagnaud, D., Barigah, T.S., Cochard, H., 2023. Concurrent time course of xylem hydraulic dysfunction and non-structural carbohydrates under contrasting water deficits and nitrogen supplies in poplar. Environ. Exp. Bot. 206, 105173.

Brunn, M., Hafner, B.D., Zwetsloot, M.J., Weikl, F., Pritsch, K., Hikino, K., Ruehr, N.K., Sayer, E.J., Bauerle, T.L., 2022. Carbon allocation to root exudates is maintained in mature temperate tree species under drought. New Phytologist 235 (3), 965–977.

Brunn, M., Krüger, J., Lang, F., 2023. Experimental drought increased the belowground sink strength towards higher topsoil organic carbon stocks in a temperate mature forest. Geoderma 431, 116356.

Brunner, I., Herzog, C., Dawes, M.A., Arend, M., Sperisen, C., 2015. How tree roots respond to drought. Front. Plant Sci. 6, 547.

Burgess, S.S., Adams, M.A., Turner, N.C., Ong, C.K., 1998. The redistribution of soil water by tree root systems. Oecologia 115 (3), 306–311.

Chiatante, D., Iorio, A.D., Sciandra, S., Scippa, G.S., Mazzoleni, S., 2006. Effect of drought and fire on root development in Quercus pubescens Willd. And Fraxinus ornus L. seedlings. Environ. Exp. Bot. 56 (2), 190–197. https://doi.org/10.1016/j.envexpbot.2005.01.014.

Chuste, P.-.A., Maillard, P., Bréda, N., Levillain, J., Thirion, E., Wortemann, R., Massonnet, C., 2020. Sacrificing growth and maintaining a dynamic carbohydrate storage are key processes for promoting beech survival under prolonged drought conditions. Trees 34 (2), 381–394. https://doi.org/10.1007/s00468-019-01923-5.

Ciais, Ph., Reichstein, M., Viovy, N., Granier, A., Ogee, J., Allard, V., Aubinet, M., Buchmann, N., Bernhofer, Chr., Carrara, A., Chevallier, F., De Noblet, N., Friend, A. D., Friedlingstein, P., Grunwald, T., Heinesch, B., Keronen, P., Knohl, A., Krinner, G., Valentini, R., 2005. Europe-wide reduction in primary productivity caused by the heat and drought in 2003. Nature 437 (7058), 529–533.

Dawadi, B., Liang, E., Tian, L., Devkota, L.P., Yao, T., 2013. Pre-monsoon precipitation signal in tree rings of timberline Betula utilis in the central Himalayas. Quatern. Int. 283, 72–77.

De Wit, H.A., Palosuo, T., Hylen, G., Liski, J., 2006. A carbon budget of forest biomass and soils in southeast Norway calculated using a widely applicable method. For. Ecol. Manage. 225 (1â€“3), 15–26. https://doi.org/10.1016/j.foreco.2005.12.023.

DeClerck, F.A., Barbour, M.G., Sawyer, J.O., 2006. Species richness and stand stability in conifer forests of the Sierra Nevada. Ecology 87 (11), 2787–2799.

Di Iorio, A., Montagnoli, A., Scippa, G.S., Chiatante, D., 2011. Fine root growth of Quercus pubescens seedlings after drought stress and fire disturbance. Environ. Exp. Bot. 74, 272–279. https://doi.org/10.1016/j.envexpbot.2011.06.009.

Ding, Y., Nie, Y., Chen, H., Wang, K., Querejeta, J.I., 2021. Water uptake depth is coordinated with leaf water potential, water-use efficiency and drought vulnerability in karst vegetation. New Phytologist 229 (3), 1339–1353. https://doi.org/10.1111/nph.16971.

Dorji, T., Brookes, J.D., Facelli, J.M., Sears, R.R., Norbu, T., Dorji, K., Chhetri, Y.R., Baral, H., 2019. Socio-cultural values of ecosystem services from Oak Forests in the Eastern Himalaya. Sustainability 11 (8), 2250.

Fan, Z., Bräuning, A., Cao, K., 2008. Tree-ring based drought reconstruction in the central Hengduan Mountains region (China) since AD 1655. Int. J. Climatol. 28 (14), 1879–1887.

FAO, 2010. Global Forest Resources Assessment: Country Report -Bhutan. Food and Agriculture Organization of the United Nations, p. 56.

Fuchs, S., Hertel, D., Schuldt, B., Leuschner, C., 2020. Effects of summer drought on the fine root system of five broadleaf tree species along a precipitation gradient. Forests 11 (3). https://doi.org/10.3390/f11030289. Article 3.

Fuchslueger, L., Bahn, M., Fritz, K., Hasibeder, R., Richter, A., 2014. Experimental drought reduces the transfer of recently fixed plant carbon to soil microbes and alters the bacterial community composition in a mountain meadow. New Phytologist 201 (3), 916–927. https://doi.org/10.1111/nph.12569.

Gaire, N.P., Bhuju, D.R., Koirala, M., Shah, S.K., Carrer, M., Timilsena, R., 2017. Tree-ring based spring precipitation reconstruction in western Nepal Himalaya since AD 1840. Dendrochronologia 42, 21–30.

Galiano, L., Martínez-Vilalta, J., Lloret, F., 2011. Carbon reserves and canopy defoliation determine the recovery of Scots pine 4yr after a drought episode. New Phytologist 190 (3), 750–759.

Gao, J., Zhang, L., Tang, Z., Wu, S., 2019. A synthesis of ecosystem aboveground productivity and its process variables under simulated drought stress. J. Ecol. 107 (6), 2519–2531.

Gaul, D., Hertel, D., Borken, W., Matzner, E., Leuschner, C., 2008. Effects of experimental drought on the fine root system of mature Norway spruce. For. Ecol. Manage. 256, 1151–1159.

Gilani, H., Shrestha, H.L., Murthy, M., Phuntso, P., Pradhan, S., Bajracharya, B., Shrestha, B., 2015. Decadal land cover change dynamics in Bhutan. J. Environ. Manage. 148, 91–100.

Godbold, D.L., Fritz, H.-.W., Jentschke, G., Meesenburg, H., Rademacher, P., 2003. Root turnover and root necromass accumulation of Norway spruce (Picea abies) are affected by soil acidity. Tree Physiol. 23 (13), 915–921.

Goebel, M.-.O., Bachmann, Jör., Reichstein, M., Janssens, I.A., Guggenberger, G., 2011. Soil water repellency and its implications for organic matter decomposition – is there a link to extreme climatic events? Glob. Chang Biol. 17 (8), 2640–2656. https://doi.org/10.1111/j.1365-2486.2011.02414.x.

Göransson, H., Godbold, D.L., Jones, D.L., Rousk, J., 2013. Bacterial growth and respiration responses upon rewetting dry forest soils: impact of drought-legacy. Soil Biol. Biochem. 57, 477–486. https://doi.org/10.1016/j.soilbio.2012.08.031.

Grierson, A.J., Long, D.G., 1983. Flora of Bhutan, Including a Record of Plants from Sikkim. Volume 1 parts 1 and 2. Royal Botanic Garden.

Gupta, P., Gupta, S., 2020. Wood anatomy of Indian oaks, with reference to systematic, ecological and evolutionary perspectives. Nord. J. Bot. 38 (4).

Hartmann, H., Moura, C.F., Anderegg, W.R.L., Ruehr, N.K., Salmon, Y., Allen, C.D., Arndt, S.K., Breshears, D.D., Davi, H., Galbraith, D., 2018. Research frontiers for improving our understanding of drought-induced tree and forest mortality. New Phytologist 218 (1), 15–28.

Jamro, G.M., Chang, S.X., Naeth, M.A., Duan, M., House, J., 2015. Fine root dynamics in lodgepole pine and white spruce stands along productivity gradients in reclaimed oil sands sites. Ecol. Evol. 5 (20), 4655–4670.

Jarvis, P., Rey, A., Petsikos, C., Wingate, L., Rayment, M., Pereira, J., Banza, J., David, J., Miglietta, F., Borghetti, M., 2007. Drying and wetting of Mediterranean soils stimulates decomposition and carbon dioxide emission: the "Birch effect. Tree Physiol. 27 (7), 929–940.

Jian, J., Vargas, R., Anderson-Teixeira, K., Stell, E., Herrmann, V., Horn, M., Kholod, N., Manzon, J., Marchesi, R., Paredes, D., 2021. A restructured and updated global soil respiration database (SRDB-V5). Earth Syst. Sci. Data 13 (2), 255–267.

Joshi, A., Joshi, P., 2019. Forest ecosystem services in the Central Himalaya: local benefits and global relevance. In: , 89, pp. 785–792.

Joshi, R.K., & Garkoti, S.C. (2021). Influence of Nepalese alder on soil physico-chemical properties and fine root dynamics in white oak forests in the central Himalaya, India. *Catena*, 200, 105140.

Joslin, J.D., Wolfe, M.H., Hanson, P., 2000. Effects of altered water regimes on forest root systems. New Phytol. 147 (1), 117–129.

Kathayat, G., Cheng, H., Sinha, A., Yi, L., Li, X., Zhang, H., Li, H., Ning, Y., Edwards, R.L., 2017. The Indian monsoon variability and civilization changes in the Indian subcontinent. Sci Adv 3 (12), e1701296.

Klein, T., 2014. The variability of stomatal sensitivity to leaf water potential across tree species indicates a continuum between isohydric and anisohydric behaviours. Funct. Ecol. 28 (6), 1313–1320.

Leonova, A., Heger, A., Vásconez Navas, L.K., Jensen, K., Reisdorff, C., 2022. Fine root mortality under severe drought reflects different root distribution of Quercus robur and Ulmus laevis trees in hardwood floodplain forests. Trees 1–11.

Leuschner, C., 2020. Drought response of European beech (Fagus sylvatica L.)—a review. Perspect. Plant Ecol. Evol. Syst. 47, 125576 https://doi.org/10.1016/j.ppees.2020.125576.

Leuzinger, S., Fatichi, S., Cusens, J., KÃ¶rner, C., Niklaus, P.A, 2015. The "island effect" in terrestrial global change experiments: a problem with no solution? AoB Plants 7. https://doi.org/10.1093/aobpla/plv092.

Limm, E.B., Simonin, K.A., Bothman, A.G., Dawson, T.E., 2009. Foliar water uptake: a common water acquisition strategy for plants of the redwood forest. Oecologia 161 (3), 449–459. https://doi.org/10.1007/s00442-009-1400-3.

Lukac, M., Godbold, D.L., 2010. Fine root biomass and turnover in southern taiga estimated by root inclusion nets. Plant Soil 331 (1), 505–513.

Mackay, D.S., Savoy, P.R., Grossiord, C., Tai, X., Pleban, J.R., Wang, D.R., McDowell, N. G., Adams, H.D., Sperry, J.S., 2020. Conifers depend on established roots during drought: results from a coupled model of carbon allocation and hydraulics. New Phytologist 225 (2), 679–692.

Makkonen, K., Helmisaari, H.S., 1999. Assessing fine-root biomass and production in a Scots pine stand-comparison of soil core and root ingrowth core methods. Plant Soil 210 (1), 43–50.

Martin-StPaul, N., Delzon, S., Cochard, H., 2017. Plant resistance to drought depends on timely stomatal closure. Ecol. Lett. 20 (11), 1437–1447.
Martin-StPaul, N.K., Limousin, J., Vogt-Schilb, H., Rodríguez-Calcerrada, J., Rambal, S., Longepierre, D., Misson, L., 2013. The temporal response to drought in a Mediterranean evergreen tree: comparing a regional precipitation gradient and a throughfall exclusion experiment. Glob. Chang Biol. 19 (8), 2413–2426.
Mayer, M., Keßler, D., Katzensteiner, K., 2020. Herbivory modulates soil CO 2 fluxes after windthrow: a case study in temperate mountain forests. Eur. J. For. Res. 139 (3), 383–391.
McDowell, N.G., Sapes, G., Pivovaroff, A., Adams, H.D., Allen, C.D., Anderegg, W.R.L., Arend, M., Breshears, D.D., Brodribb, T., Choat, B., Cochard, H., De Cáceres, M., De Kauwe, M.G., Grossiord, C., Hammond, W.M., Hartmann, H., Hoch, G., Kahmen, A., Klein, T., Xu, C., 2022. Mechanisms of woody-plant mortality under rising drought, CO2 and vapour pressure deficit. Nature Rev. Earth Environ. 3 (5) https://doi.org/10.1038/s43017-022-00272-1. Article 5.
McDowell, N., Pockman, W.T., Allen, C.D., Breshears, D.D., Cobb, N., Kolb, T., Plaut, J., Sperry, J., West, A., Williams, D.G., 2008. Mechanisms of plant survival and mortality during drought: why do some plants survive while others succumb to drought? New Phytologist 178 (4), 719–739.
McGregor, I.R., Helcoski, R., Kunert, N., Tepley, A.J., Gonzalez-Akre, E.B., Herrmann, V., Zailaa, J., Stovall, A.E.L., Bourg, N.A., McShea, W.J., Pederson, N., Sack, L., Anderson-Teixeira, K.J., 2021. Tree height and leaf drought tolerance traits shape growth responses across droughts in a temperate broadleaf forest. New Phytologist 231 (2), 601–616. https://doi.org/10.1111/nph.16996.
Meier, I.C., Leuschner, C., 2008. Genotypic variation and phenotypic plasticity in the drought response of fine roots of European beech. Tree Physiol. 28 (2), 297–309.
Meinzer, F.C., Warren, J.M., Brooks, J.R., 2007. Species-specific partitioning of soil water resources in an old-growth Douglas-fir–western hemlock forest. Tree Physiol. 27 (6), 871–880.
Menon, A., Levermann, A., Schewe, J., Lehmann, J., Frieler, K., 2013. Consistent increase in Indian monsoon rainfall and its variability across CMIP-5 models. Earth Syst. Dyn. Discuss. 4 (1), 1–24. https://doi.org/10.5194/esdd-4-1-2013.
Michaelian, M., Hogg, E.H., Hall, R.J., Arsenault, E., 2011. Massive mortality of aspen following severe drought along the southern edge of the Canadian boreal forest. Glob. Chang Biol. 17 (6), 2084–2094.
Minore, D. (1983). *Western redcedar: a literature review*.
Moser, G., Schuldt, B., Hertel, D., Horna, V., Coners, H., Barus, H., Leuschner, C., 2014. Replicated throughfall exclusion experiment in an Indonesian perhumid rainforest: wood production, litter fall and fine root growth under simulated drought. Glob. Chang Biol. 20 (5), 1481–1497.
Nikolova, P.S., Bauerle, T.L., Häberle, K.-.H., Blaschke, H., Brunner, I., Matyssek, R., 2020. Fine-root traits reveal contrasting ecological strategies in european beech and norway spruce during extreme drought. Front. Plant Sci. 11, 1211.
Ohsawa, M., 1987. Life Zone Ecology of the Bhutan Himalaya. Laboratory of Ecology, Chiba University Chiba, Japan.
Oishi, A.C., Oren, R., Novick, K.A., Palmroth, S., Katul, G.G., 2010. Interannual invariability of forest evapotranspiration and its consequence to water flow downstream. Ecosystems 13 (3), 421–436. https://doi.org/10.1007/s10021-010-9328-3.
Oliveira, R.G., Noordwijk, M.van, Gaze, S., Brouwer, G., Bona, S., Mosca, G., Hairiah, K, 2000. Auger sampling, ingrowth cores and pinboard methods. Root Methods. Springer, pp. 175–210.
Ouyang, S.-.N., Gessler, A., Saurer, M., Hagedorn, F., Gao, D.-.C., Wang, X.-.Y., Schaub, M., Li, M.-.H., Shen, W.-.J., Schönbeck, L., 2021. Root carbon and nutrient homeostasis determines downy oak sapling survival and recovery from drought. Tree Physiol.
Panthi, S., Bräuning, A., Zhou, Z.-.K., Fan, Z.-.X., 2017. Tree rings reveal recent intensified spring drought in the central Himalaya, Nepal. Glob. Planet. Change 157, 26–34. https://doi.org/10.1016/j.gloplacha.2017.08.012 (Supplement C),.
Pardos, M., del Río, M., Pretzsch, H., Jactel, H., Bielak, K., Bravo, F., Brazaitis, G., Defossez, E., Engel, M., Godvod, K., 2021. The greater resilience of mixed forests to drought mainly depends on their composition: analysis along a climate gradient across Europe. For. Ecol. Manage. 481, 118687.
Pinheiro, J., Bates, D., DebRoy, S., Sarkar, D., & Team, R.C. (2014). Nlme: linear and nonlinear mixed effects models. R package version 3.1-117. *R Core Team (2014)*.
Pinheiro, J.C., Bates, D.M., 2000. Mixed-Effects Models in S and S-Plus. Springer - Verlag.
Piper, F.I., Paula, S., 2020. The role of nonstructural carbohydrates storage in forest resilience under climate change. Curr. Forest. Rep. 6 (1), 1–13.
Poudyal, K., Jha, P., Zobel, D., Thapa, C., 2004. Patterns of leaf conductance and water potential of five Himalayan tree species. Tree Physiol. 24 (6), 689–699.
Preethi, B., Ramya, R., Patwardhan, S., Mujumdar, M., Kripalani, R., 2019. Variability of Indian summer monsoon droughts in CMIP5 climate models. Clim. Dyn. 53 (3), 1937–1962.
R Core Team, 2017. R Foundation for Statistical Computing. R: A language and environment for statistical computing, Vienna, Austria, 2018.
Reichstein, M., Beer, C., 2008. Soil respiration across scales: the importance of a model–data integration framework for data interpretation. J. Plant Nutr. Soil Sci. 171 (3), 344–354.
Rousk, J., Smith, A.R., Jones, D.L., 2013. Investigating the long-term legacy of drought and warming on the soil microbial community across five E uropean shrubland ecosystems. Glob. Chang Biol. 19 (12), 3872–3884.
Rovira, P., Rovira, R., 2010. Fitting litter decomposition datasets to mathematical curves: towards a generalised exponential approach. Geoderma 155 (3–4), 329–343.
Sánchez-García, C., Doerr, S.H., Urbanek, E., 2020. The effect of water repellency on the short-term release of CO2 upon soil wetting. Geoderma 375, 114481.
Schewe, J., Levermann, A., 2012. A statistically predictive model for future monsoon failure in India. Environ. Res. Lett. 7 (4), 044023.
Schimel, J.P., 2018. Life in dry soils: effects of drought on soil microbial communities and processes. Annu. Rev. Ecol. Evol. Syst. 49, 409–432.
Schindlbacher, A., Wunderlich, S., Borken, W., Kitzler, B., Zechmeister-Boltenstern, S., Jandl, R., 2012. Soil respiration under climate change: prolonged summer drought offsets soil warming effects. Glob. Chang. Biol. 18, 2270–2279.
Schreel, J.D.M., Steppe, K., 2020. Foliar water uptake in trees: negligible or necessary? Trends Plant Sci. 25 (6), 590–603. https://doi.org/10.1016/j.tplants.2020.01.003.
Sharma, P., Rai, S.C., 2007. Carbon sequestration with land-use cover change in a Himalayan watershed. Geoderma 139 (3–4), 371–378. https://doi.org/10.1016/j.geoderma.2007.02.016.
Simon, A., Dhendup, K., Rai, P.B., Gratzer, G., 2018. Soil carbon stocks along elevational gradients in Eastern Himalayan mountain forests. Geoderma Region. 12, 28–38. https://doi.org/10.1016/j.geodrs.2017.11.004.
Singh, D., Ghosh, S., Roxy, M.K., McDermid, S., 2019. Indian summer monsoon: extreme events, historical changes, and role of anthropogenic forcings. Wiley Interdiscip. Rev. 10 (2), e571.
Singh, D., Tsiang, M., Rajaratnam, B., Diffenbaugh, N.S., 2014. Observed changes in extreme wet and dry spells during the South Asian summer monsoon season. Nat. Clim. Chang 4 (6), 456–461.
Singh, N., Parida, B.R., 2019. Environmental factors associated with seasonal variations of night-time plant canopy and soil respiration fluxes in deciduous conifer forest, Western Himalaya, India. Trees 33 (2), 599–613.
Sokol, N.W., Kuebbing, Sara.E., Karlsen-Ayala, E., Bradford, M.A., 2019. Evidence for the primacy of living root inputs, not root or shoot litter, in forming soil organic carbon. New Phytologist 221 (1), 233–246. https://doi.org/10.1111/nph.15361.
Song, Y., Sass-Klaassen, U., Sterck, F., Goudzwaard, L., Akhmetzyanov, L., Poorter, L., 2021. Growth of 19 conifer species is highly sensitive to winter warming, spring frost and summer drought. Ann. Bot. 128 (5), 545–557.
Tashi, S., Singh, B., Keitel, C., Adams, M., 2016. Soil carbon and nitrogen stocks in forests along an altitudinal gradient in the eastern Himalayas and a meta-analysis of global data. Glob. Chang Biol. 22, 2255–2268. https://doi.org/10.1111/gcb.13234.
Thomas, F.M., Gausling, T., 2000. Morphological and physiological responses of oak seedlings (*Quercus petraea* and *Q. robur*) to moderate drought. Ann. For. Sci. 57 (4), 325–333. https://doi.org/10.1051/forest:2000123.
Trugman, A.T., Detto, M., Bartlett, M.K., Medvigy, D., Anderegg, W.R.L., Schwalm, C., Schaffer, B., Pacala, S.W., 2018. Tree carbon allocation explains forest drought—kill and recovery patterns. Ecol. Lett. 21 (10), 1552–1560.
Upadhyay, V., Rana, B., Mishra, R., 2003. Fine root productivity of two central himalayan forest ecosystems. Plant Sci. Res. 25, 21–25.
van der Molen, M.K., Dolman, A.J., Ciais, P., Eglin, T., Gobron, N., Law, B.E., Meir, P., Peters, W., Phillips, O.L., Reichstein, M., Chen, T., Dekker, S.C., Doubkova, M., Friedl, M.A., Jung, M., van den Hurk, B.J.J.M., de Jeu, R.A.M., Kruijt, B., Ohta, T., Wang, G., 2011. Drought and ecosystem carbon cycling. Agric. For. Meteorol. 151 (7), 765–773. https://doi.org/10.1016/j.agrformet.2011.01.018.
van Straaten, O., Veldkamp, E., Corre, M.D., 2011. Simulated drought reduces soil CO2 efflux and production in a tropical forest in Sulawesi, Indonesia. Ecosphere 2 (10), 1–22.
Vanhellemont, M., Sousa-Silva, R., Maes, S.L., Van den Bulcke, J., Hertzog, L., De Groote, S.R., Van Acker, J., Bonte, D., Martel, A., Lens, L., 2019. Distinct growth responses to drought for oak and beech in temperate mixed forests. Sci. Total Environ. 650, 3017–3026.
Vanoni, M., Bugmann, H., Nötzli, M., Bigler, C., 2016. Quantifying the effects of drought on abrupt growth decreases of major tree species in Switzerland. Ecol. Evol. 6 (11), 3555–3570.
Wangchuk, J., Choden, K., Sears, R.R., Baral, H., Yoezer, D., Tamang, K.T.D., Choden, T., Wangdi, N., Dorji, S., Dukpa, D., 2021. Community perception of ecosystem services from commercially managed forests in Bhutan. Ecosyst. Serv. 50, 101335.
Wangda, P., Ohsawa, M., 2006. Gradational forest change along the climatically dry valley slopes of Bhutan in the midst of humid eastern Himalaya. Plant Ecol. 186 (1), 109–128. https://doi.org/10.1007/s11258-006-9116-5.
Wangdi, N., Mayer, M., Nirola, M.P., Zangmo, N., Orong, K., Ahmed, I.U., Darabant, A., Jandl, R., Gratzer, G., Schindlbacher, A., 2017a. Soil CO2 efflux from two mountain forests in the eastern Himalayas, Bhutan: components and controls. Biogeosciences 14 (1), 99–110.
Wangdi, N., Om, K., Thinley, C., Drukpa, D., Dorji, T., Darabant, A., Chhetri, P.B., Ahmed, I.U., Staudhammer, C.L., Jandl, R., 2017b. Climate change in remote mountain regions: a throughfall-exclusion experiment to simulate monsoon failure in the Himalayas. Mount Res. Dev. 37 (3), 294–309.
Werner, C., Meredith, L.K., Ladd, S.N., Ingrisch, J., Kübert, A., van Haren, J., Bahn, M., Bamberger, I., Beyer, M., Blomdahl, D., 2021. Ecosystem fluxes during drought and recovery in an experimental forest. Science 374 (6574), 1514–1518.
Wikramanayake, E.D., 2002. Terrestrial Ecoregions of the Indo-Pacific: A conservation Assessment. Island Press.
Williams, A., de Vries, F.T., 2020. Plant root exudation under drought: implications for ecosystem functioning. New Phytologist 225 (5), 1899–1905. https://doi.org/10.1111/nph.16223.
WRB, I.W.G., 2006. World Reference Base for Soil Resources 2006. FAO.
Xu, B., Arain, M.A., Black, T.A., Law, B.E., Pastorello, G.Z., Chu, H., 2020. Seasonal variability of forest sensitivity to heat and drought stresses: a synthesis based on

carbon fluxes from North American forest ecosystems. Glob. Chang Biol. 26 (2), 901–918. https://doi.org/10.1111/gcb.14843.

Yang, Y., Liu, S., Schindlbacher, A., Wang, J., Li, Z., Wang, H., Ming, A., Lu, L., Li, Z., 2021. Topsoil organic carbon increases but its stability declines after five years of reduced throughfall. Soil Biol. Biochem. 156, 108221 https://doi.org/10.1016/j.soilbio.2021.108221.

Zwetsloot, M.J., Bauerle, T.L., 2021. Repetitive seasonal drought causes substantial species-specific shifts in fine-root longevity and spatio-temporal production patterns in mature temperate forest trees. New Phytologist 231 (3), 974–986.